ISSN 1054-660X, Laser Physics, 2012, Vol. 22, No. 11, pp. 1721–1728.

>100-kW Linearly Polarized Pulse Fiber Amplifier Seeded by a Compact Efficient Passively *Q*-switched Nd:YVO_4 Laser[1]

W. Z. Zhuang, W. C. Huang, C. Y. Cho, Y. P. Huang, J. Y. Huang, and Y. F. Chen*

Department of Electrophysics, National Chiao Tung University, 1001 Ta Hsueh Road, Hsinchu, 30010, Taiwan

*e-mail: yfchen@cc.nctu.edu.tw

Received December 21, 2012; in final form, December 28, 2012; published online October 1, 2012

Abstract—We thoroughly develop compact high-peak-power Nd:YVO_4/Cr^{4+}:YAG passively *Q*-switched lasers (PQS) as the seed source of the fiber amplifier. We exploit a nearly hemispherical cavity to reach the second threshold criterion and systematically consider the thermal lensing effect and the mode-size matching in the overall optimization. Employing a Cr^{4+}:YAG absorber with 70% initial transmission, we obtain a 50-kHz seed pulse train with the pulse duration of 4.8 ns and the pulse energy of 22 μJ at a pump power of 5.4 W. Injecting this seed laser into a polarization maintained Yb-doped fiber, the pulse energy and peak power at a pump power of 16 W are enhanced up to 178 μJ and 37 kW, respectively. We also use an absorber with 40% initial transmission to generate a 25 kHz pulse train with the pulse duration of 1.6 ns and the pulse energy of 36 μJ at a pump power of 5.4 W. With this seed laser, we find that the surface damage of the fiber limits the maximum pulse energy and peak power to be 192 μJ and 120 kW, respectively.

DOI: 10.1134/S1054660X12110205

1. INTRODUCTION

High-peak-power, linearly-polarized lasers with pulse repetition rates up to several tens of kilohertz have a wide variety of applications in range finding, nonlinear wavelength conversion, and material processing [1–3]. The thermally induced distortion is the main hindrance for power scale-up in solid-state crystal lasers [4]. The master-oscillator fiber power-amplifier (MOFA) that collects the advantages of good beam quality, high efficiency, compactness, and superior heat dissipations has been identified as a promising light source [5–9]. To achieve the high-peak-power pulses with single-stage amplification, diode-pumped actively *Q*-switched (AQS) [10, 11] or passively *Q*-switched (PQS) [12–14] Nd-doped lasers are often used as the seed lasers of the Yb-doped MOFAs.

Compared to the active *Q*-switching, the PQS laser with a saturable absorber offers the advantages of compactness, robustness, and low cost. Since Cr^{4+}:YAG crystals possess the advantages of high absorption cross section near the infrared region, high damage threshold, and low temperature-sensitive properties [15–21], they have been proved to be reliable saturable absorbers for Nd^{3+}-doped lasers. Nevertheless, the Cr^{4+}:YAG crystal is usually not convenient for the Nd-doped vanadate crystal lasers due to the mismatch between the stimulated emission cross section of the gain medium and the absorption cross section of the absorber. Several methods, including the three-element resonator with the intra-cavity focusing [15, 20, 22] or the employment of a *c*-cut crystal as the gain medium [23–25], have been proposed to overcome this mismatch. The three-element resonators, however, not only increase the complexity of the cavities but also lead to relatively long pulse durations owing to the long cavity lengths. On the other hand, the employment of a *c*-cut crystal inevitably raises the pumping threshold and loses the characteristic of linear polarization. Therefore, it is highly useful for the seed laser of MOFA to develop high-peak-power PQS lasers with *a*-cut vanadate crystals in a simple compact cavity.

In this work, we systematically consider the second threshold criterion and the thermal lensing effect to develop compact and high-peak-power Nd:YVO_4/Cr^{4+}:YAG PQS lasers with nearly hemispherical cavities. We further exploit several Cr^{4+}:YAG crystals with different initial transmissions (T_0) to realize the designed PQS laser. Experimental results reveal that at a pump power of 5.4 W the output pulse energy increases from 22 to 36 μJ and the pulse repetition rate decreases from 50 to 25 kHz for the initial transmission of the Cr^{4+}:YAG crystal decreasing form 70% to 40%. Injecting the seed laser obtained with $T_0 = 70\%$ into a polarization maintained Yb-doped fiber, the pulse energy and peak power at a pump power of 16 W are enhanced up to 178 μJ and 37 kW, respectively. Excellent amplification confirms the PQS performance. Employing the seed laser obtained with $T_0 = 40\%$, we find that the surface damage of the fiber limits the maximum pulse energy and peak power to be 192 μJ and 120 kW, respectively. The polarization extinction ratio is approximately 100:1 for both MOFAs in the whole pump power. To the best of our knowledge, this is the first time to realize high-peak-power, single-stage, linearly-polarized MOFAs with the compact Nd:YVO_4/Cr^{4+}:YAG PQS lasers as seed oscillators.

[1] The article is published in the original.

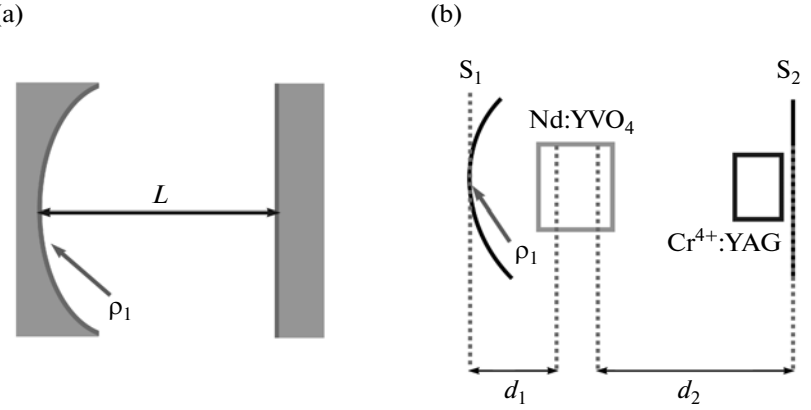

Fig. 1. (a) Schematic diagram of the plano-concave cavity. (b) Equivalent cavity diagram of the Nd:YVO_4/Cr^{4+}:YAG PQS laser.

2. ANALYSIS AND OPTIMIZATION OF THE PQS LASER

To achieve good passive *Q*-switching, absorption saturation in the absorber must occur before gain saturation in the laser crystal [22]. From the analysis of the coupled rate equation, the good passively *Q*-switching criterion which is also called second threshold condition is given by:

$$\frac{\ln(1/T_0^2)}{\ln(1/T_0^2)+\ln(1/R)+L}\frac{\sigma_{gsa}}{\sigma}\frac{A}{A_s} > \frac{\gamma}{1-\beta}, \quad (1)$$

where R is the reflectivity of the output coupler, σ is the stimulated emission cross-section of the gain medium, σ_{gsa} is the ground-state absorption cross-section of the saturable absorber with the initial transmission T_0, L is the nonsaturable intracavity round-trip dissipative optical loss, A/A_s is the ratio of the effective area in the gain medium to that in the saturable absorber, γ is the inversion reduction factor with a value between 0 and 2 [26], and β is the ratio of the excited-state absorption cross-section to that of the ground-state absorption in the saturable absorber. The challenge of obtaining a compact and stable Nd:YVO_4/Cr^{4+}:YAG PQS laser results from which the emission cross-section of Nd:YVO_4 crystals (~2.5×10^{-18} cm^2) [15] is comparable with the ground-state absorption cross-section of Cr^{4+}:YAG crystals (~$(2.0 \pm 0.5) \times 10^{-18}$ cm^2) [27]. It was found that unstable pulse trains with satellite pulses would occur when the good *Q*-switching criterion is not achieved [28, 29]. To fulfill the good passive *Q*-switching criterion in Nd:YVO_4/Cr^{4+}:YAG PQS lasers, the ratio A/A_s generally needs to be greater than 10 [29].

Even though the three-element resonator can be used to achieve the requirement of the ratio $A/A_s \geq 10$, the long cavity usually leads to a wide pulse duration. Here we utilize the nearly hemispherical resonator to develop compact high-peak-power Nd:YVO_4/Cr^{4+}:YAG PQS lasers to be seed oscillators. In terms of the *g*-parameters, the beam radii ω_1 and ω_2 on the rear and front mirrors are given by [30]:

$$g_i = 1 - \frac{L}{\rho_i}, \quad (2)$$

$$\omega_i = \sqrt{\frac{\lambda L}{\pi}\sqrt{\frac{g_j}{g_i(1-g_1g_2)}}}; \quad i,j = 1,2; \quad i \neq j, \quad (3)$$

where L is the cavity length, λ is the wavelength of laser mode, and ρ_1 and ρ_2 are the radii of curvature of the rear and front mirrors, respectively. For a simple plano-concave resonator, as depicted in Fig. 1a, $g_1 = 1 - L/\rho_1$ and $g_2 = 1$. Given that the gain medium and the saturable absorber are as close as possible to the rear mirror and the flat output coupler, the ratio of the effective area in the gain medium to that in the saturable absorber A/A_s can be found to be

$$\frac{A}{A_s} = \frac{\omega_1^2}{\omega_2^2} = \frac{\rho_1}{\rho_1 - L}. \quad (4)$$

Equation (4) reveals that the ratio A/A_s can be up to 10 under the circumstance of a nearly hemispherical cavity with $L = 0.9\rho_1$. A smaller ρ_1 consequently corresponds to a shorter cavity length that is beneficial for the generation of *Q*-switched pulses with narrower pulse duration. Nevertheless, the geometrical sizes of the gain medium, the saturable absorber, and the heat sinks limit the minimum cavity length. Therefore, $\rho_1 =$ 25 mm is chosen for further optimizing the compact high-peak-power Nd:YVO_4/Cr^{4+}:YAG PQS laser.

The next design parameter is the pump size that needs to be optimized to reach the good mode matching for the fundamental transverse mode. Since the thermal lensing effect in the gain medium always affects the cavity mode size, it is practically important to consider the thermal lensing effect for determining the optimum pump size. For an end-pumped crystal laser, the thermal lens is given by [31]:

$$\frac{1}{f_{th}} = \frac{\xi P_{in}}{\pi K_c}\int_0^l \frac{\alpha e^{-\alpha z}}{1-e^{-\alpha l}}\frac{1}{\omega_p^2(z)}\left[\frac{1}{2}\frac{dn}{dT} + (n-1)\alpha_T\frac{\omega_p(z)}{l}\right]dz, \quad (5)$$

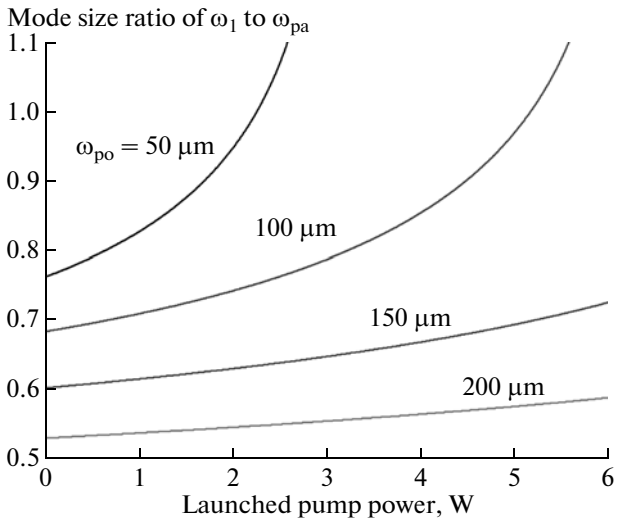

Fig. 2. Dependence of the mode-to-pump size ratio ω_1/ω_{pa} on the pump power for different pumping spot radii.

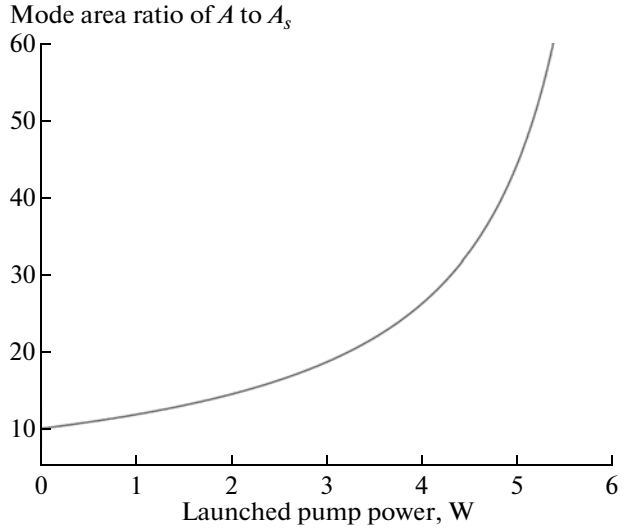

Fig. 3. Effective mode area ratio of A/A_s as a function of the pump power in the Nd:YVO_4/Cr^{4+}:YAG PQS laser with $L = 0.9\rho_1$, $\rho_1 = 25$ mm, $\omega_p = 100$ μm.

where

$$\omega_p(z) = \omega_{po}\sqrt{1+\left[\frac{\lambda_p M_p^2(z-z_o)}{n\pi\omega_{po}^2}\right]^2}, \quad (6)$$

z_0 is the focal plane of the pump beam in the laser crystal, M_p^2 is the pump beam quality factor, ω_{po} is the pump beam radius, n is the refractive index of along the c-axis of the laser crystal, λ_p is the wavelength of the pump laser diode, ξ is the fractional thermal loading, K_c is the thermal conductivity, P_{in} is the incident pump power, α is the absorption coefficient of the gain medium, l is the crystal length, dn/dT is the thermal-optic coefficient of n, and α_T is the thermal expansion coefficient along the a-axis.

Figure 1b depicts the configuration of a nearly hemispherical resonator for a Nd:YVO_4/Cr^{4+}:YAG PQS laser. Considering the thermal lens effect and taking S_1 as the reference plane, the ray transfer matrix from S_1 to S_2 of the cavity configuration can be presented as [32]:

$$M_D = \begin{pmatrix} g_1^* & L^* \\ \dfrac{g_1^* g_2^* - 1}{L^*} & g_2^* \end{pmatrix}, \quad (7)$$

$$g_i^* = g_i - \frac{d_j}{f_{\text{th}}}\left(1 - \frac{d_i}{\rho_i}\right), \quad (8)$$

$$g_i = 1 - \frac{d_1 + d_2}{\rho_i}; \quad i,j = 1,2;\ i \neq j, \quad (9)$$

$$L^* = d_1 + d_2 - \frac{d_1 d_2}{f_{\text{th}}}. \quad (10)$$

Here d_1 and d_2 are the optical path length between the cavity mirrors and the principal planes of the laser crystal, and f_{th} is the effective focal length of the thermal lens. With the following parameters: $\xi = 0.24$, $K_c = 5.23$ W/K m, $d_1 = 2$ mm, $d_2 = 0.9\rho_1 - d_1$, $\rho_2 = \infty$, $n = 2.165$, $l = 12$ mm, $dn/dT = 3.0 \times 10^{-6}$ K^{-1}, $M_p^2 = 80$, $\alpha = 0.6$ mm^{-1}, $\alpha_T = 4.43 \times 10^{-6}$ K^{-1}, and $\lambda_p = 808$ nm, the effective focal length of the thermal lens effect and g^*-parameters of the resonator can be calculated as functions of the incident pump power. In terms of the g^*-parameters for the thermal lensing effect, the beam radii ω_1 and ω_2 on the rear and front mirrors can be expressed as [32]:

$$\omega_i = \sqrt{\frac{\lambda L^*}{\pi}}\sqrt{\frac{g_j^*}{g_i^*(1 - g_1^* g_2^*)}}; \quad i,j = 1,2; \quad i \neq j. \quad (11)$$

Figure 2 shows the mode-to-pump size ratio ω_1/ω_{pa} of different pumping spot radii as a function of the pump power with the radius of curvature of the rear mirror of 25 mm, where the averaged pump size along the gain medium is given by [33]:

$$\omega_{pa} = \int_0^l \omega_p(z) e^{-\alpha z} dz \Big/ \int_0^l e^{-\alpha z} dz. \quad (12)$$

According to the optimal mode matching condition [33], the ratio of ω_1/ω_{pa} should be in the range of 0.8 to 1.2 for $P_{\text{in}} < 10$ W. In our design, the maximum pump power is approximately 5.5 W. As can be seen from the Fig. 2, the optimum pump radius is in the region of 100 μm.

With $\omega_{po} = 100$ μm and $\rho_1 = 25$ mm, we consider the thermal lensing effect to calculate the effective mode area ratio of A/A_s as a function of the pump power. Fig-

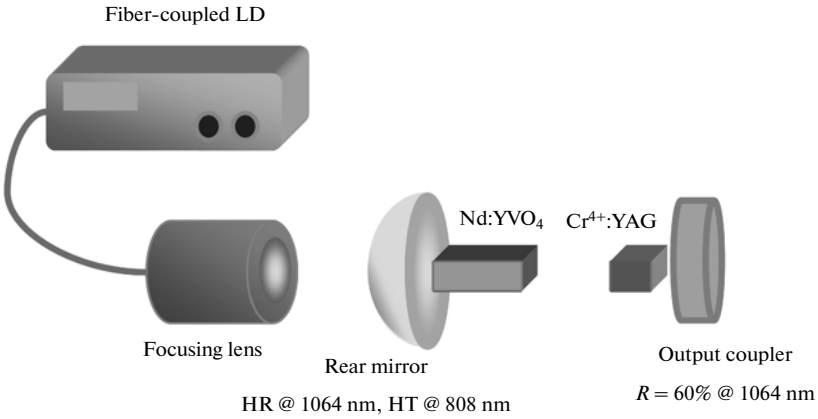

Fig. 4. Schematic diagram of a diode-pumped Nd:YVO_4 laser PQS with a Cr^{4+}:YAG as a saturable absorber. HR—high reflection. HT—high transmission.

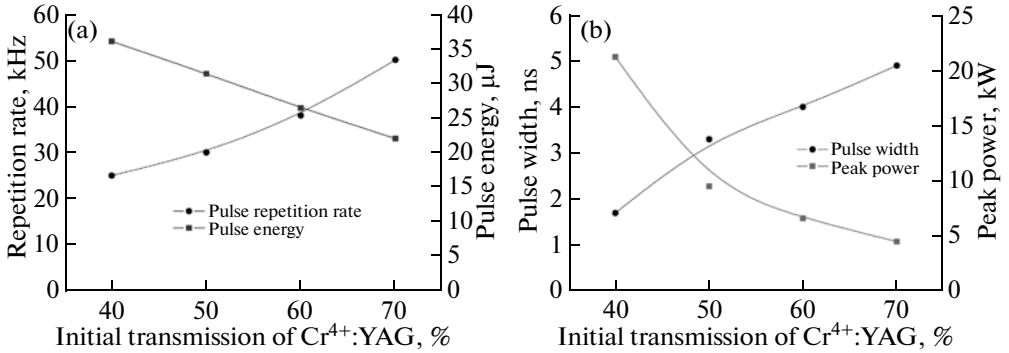

Fig. 5. (a) Dependence of the pulse repetition rate and the pulse energy on the initial transmission of Cr^{4+}:YAG at the pump power of 5.4 W. (b) Dependence of the pulse width and the peak power on the initial transmission of Cr^{4+}:YAG at the pump power of 5.4 W.

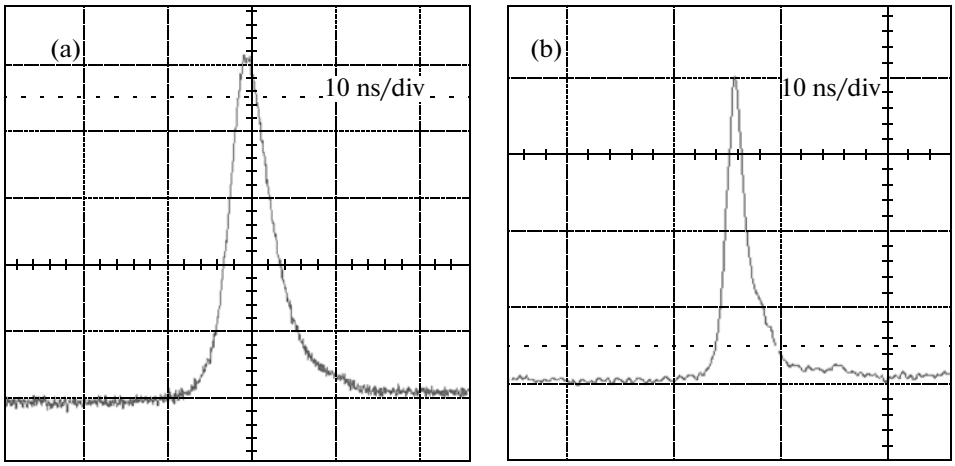

Fig. 6. Oscilloscope traces of a single pulse of (a) PQS laser with Cr^{4+}:YAG of $T_0 = 70\%$, (b) PQS laser with Cr^{4+}:YAG of $T_0 = 40\%$.

ure 3 shows the calculated result for the dependence of the effective mode area ratio of A/A_s on the pump power. It can be seen that the effective mode area ratio of A/A_s is generally greater than 10 for the pump power less than 5.5 W. To be brief, we choose a nearly hemispherical cavity with the radius of curvature of the rear

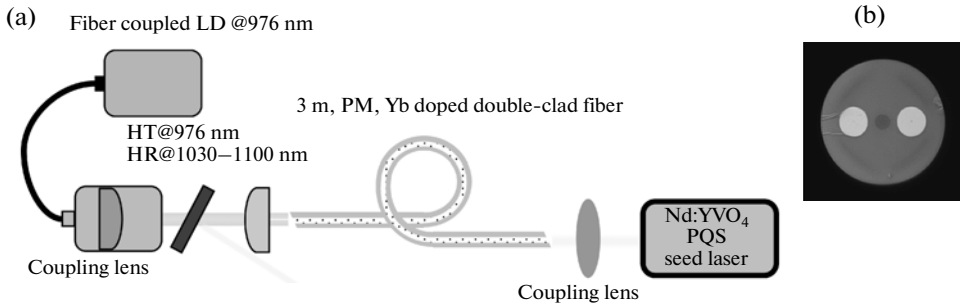

Fig. 7. (a) Scheme of the MOFA setup. HT: high transmission HR: high reflection. (b) Cross section of the PM Yb-doped fiber.

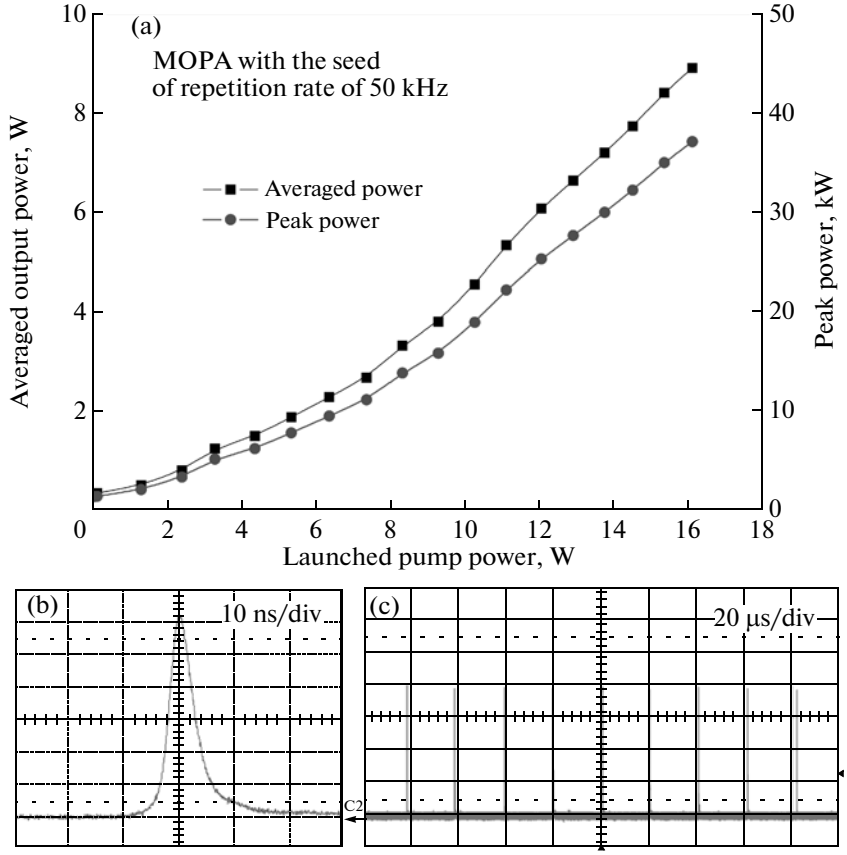

Fig. 8. (a) Average output power and peak power of MOFA with the seed of repetition rate of 50 kHz as a function of the launched pump power. (b) Oscilloscope traces of a single pulse of the output pulse of the amplifier. (c) Oscilloscope traces of a train of amplified pulses.

mirror of 25 mm and the pumping spot radius of 100 μm to simultaneously satisfy the optimal mode matching condition and the good Q-switching criterion.

3. EXPERIMENTAL RESULTS FOR THE PQS LASER

We followed the theoretical analysis to construct a nearly hemispherical cavity for realizing the compact high-peak-power Nd:YVO_4/Cr^{4+}:YAG PQS laser, as shown in Fig. 4 for the experimental setup. The rear mirror was a concave mirror with a radius-of-curvature of 25 mm with high-transmission coating at 808 nm ($T \sim 95\%$) and high-reflection at 1064 nm ($R > 99.8\%$). The output coupler was a flat mirror with partially reflection at 1064 nm ($R = 60\%$). The pumping source was a 7-W 808-nm fiber-coupled laser diode with a core diameter of 200 μm and a numerical aperture of 0.22. The focusing lens with 25 mm focal length and 80% coupling efficiency was used to re-

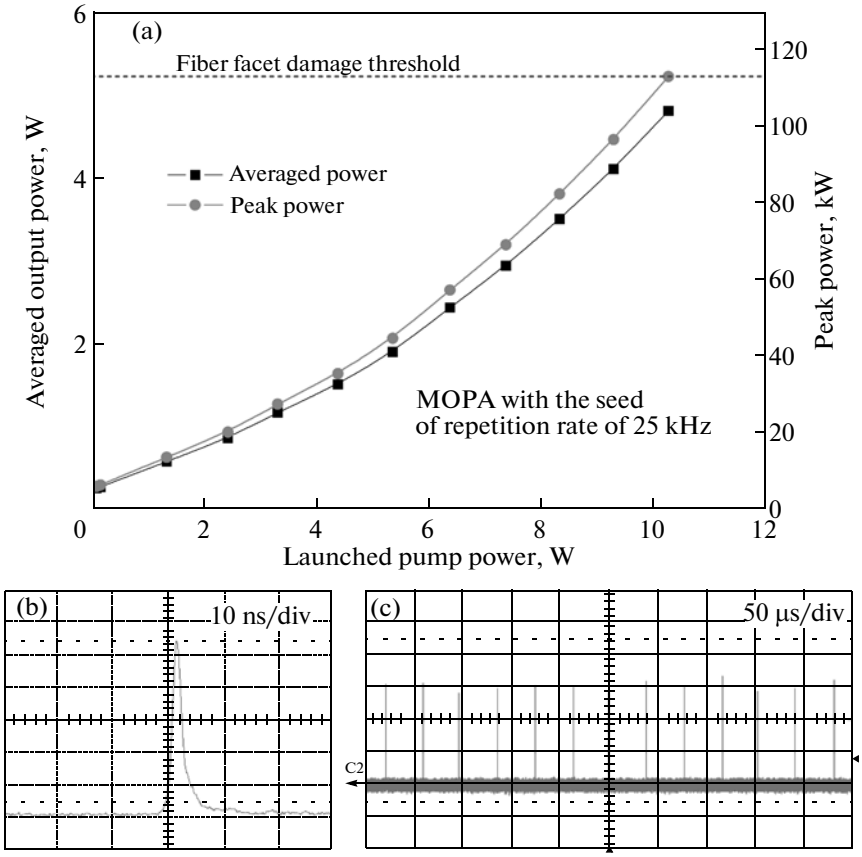

Fig. 9. (a) Average output power and peak power of MOFA with the seed of repetition rate of 25 kHz as a function of the launched pump power. (b) Oscilloscope traces of a single pulse of the output pulse of the amplifier. (c) Oscilloscope traces of a train of amplified pulses.

image the pump beam into the laser crystal. The gain medium was an *a*-cut 12-mm-long Nd:YVO_4 crystal with 0.3 at % Nd^{3+} concentration. Several Cr^{4+}:YAG absorbers with T_0 of 70, 60, 50%, and 40% were used to investigate the performance. The Cr^{4+}:YAG crystals were all 2 mm in thickness. Both sides of the Nd:YVO_4 and the Cr:YAG crystals were coated for antireflection at 1064 nm. All the laser crystal were wrapped within indium foils and mounted in the water cooled heat sinks that keep at 19°C. The Nd:YVO_4 crystal and Cr^{4+}:YAG crystals were placed as close as possible to the rear mirror and the output coupler respectively. The effective cavity length was set to be 22.5 mm based on the design rule of $L = 0.9\rho_1$. The pulse temporal behavior was recorded by Leroy digital oscilloscope (Wavepro 7100; 10G samples/s; 4 GHz bandwidth) with a fast InGaAs photodiode.

Figure 5a shows the output pulse energies and pulse repetition rates for Cr^{4+}:YAG saturable absorbers with different initial transmissions T_0 at the pump power of 5.4 W. It can be seen that for the initial transmission T_0 decreasing form 70 to 40% the output pulse energy increases from 22 to 36 μJ; at the same time, the pulse repetition rate decreases from 50 to 25 kHz. Figure 5b depicts the pulse widths and peak powers for saturable absorbers with different initial transmissions T_0 at the pump power of 5.4 W. For the initial transmission T_0 decreasing form 70 to 40% the pulse width can be seen to decrease from 4.8 ns to 1.6 ns; consequently, the peak power was enhanced from 4.5 to 22.5 kW. Figures 6a and 6b show typical oscilloscope traces for a single pulse at the maximum output powers of the seeds with $T_0 = 70$ and 40%, respectively. Experimental results reveal that the characteristics of the output pulse in the present PQS laser display a simple pulse train without the satellite pulses phenomenon. It is worth mentioning that the satellite pulses phenomena such as two pulses oscillate simultaneously or one giant pulse followed by a weak pulse are often observed when the laser cavity does not properly comply with the second threshold criterion in Eq. (1). The spectral spectrum was measured by an optical spectrum analyzer with 0.1-nm resolution (Advantest Q8381A). The spectral linewidths for all the present PQS lasers were nearly the same to be 0.5 nm. In the next section, we will employ these high-peak-power PQS lasers to realize a single stage, linear-polarized fiber amplifier.

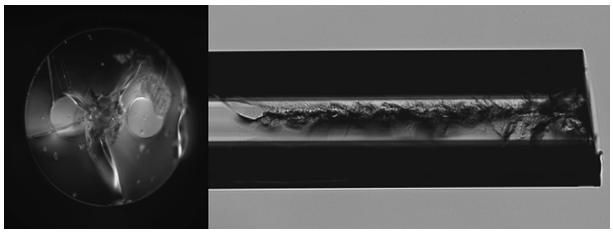

Fig. 10. End view and side view of the damaged fiber.

4. EXPERIMENTAL RESULTS FOR THE MOFA SYSTEM

The experimental architecture for the MOFA system is shown in Fig. 7a. The gain fiber was a 3-m-long Yb-doped Panda-style PM double clad fiber (Nufern) with a core diameter of 30 μm (N.A. = 0.06) and an inner clad diameter of 250 μm (N.A. = 0.46) with pump absorption of 6.6 dB/m at 975 nm. The Panda-style stress applying parts around the core generate a birefringence of 1.5×10^{-4}. A microscope image of the fiber cross-section is depicted in Fig. 7b. Both ends of the fiber were polished at an angle of 8° to eliminate the end facet reflection. The pump source was a 20-W 976-nm fiber-coupled laser diode with a core diameter of 200 μm and a numerical aperture of 0.2. A focusing lens with 25-mm focal length was used to re-image the pump beam into the fiber through a dichroic mirror with high transmission (HT, $T > 90\%$) at 976 nm and high reflectivity (HR, $R > 99.8\%$) within 1030–1100 nm. The pump spot radius was approximately 100 μm, and the pump coupling efficiency was estimated to be nearly 80%. The seed laser was coupled through a focusing lens into the core of the fiber. A half-wave plate was used to control the polarization direction of the seed laser to match the fast-axis of the PM fiber.

Figure 8a shows the average output power of the MOFA injected by the seed laser with $T_0 = 70\%$ as a function of launched pump power at a repetition rate of 50 kHz. Under the launched pump power of 16 W, the output power of the amplifier was 8.9 W, corresponding to the pulse energy of 178 μJ. The slope efficiency was approximately 54%. Figure 8b shows the typical oscilloscope trace for a single pulse at the maximum output power of amplifier. The pulse duration was 4.8 ns and the corresponding peak power was 37 kW. The oscilloscope trace of a train of output pulses of the amplifier is shown in Fig. 8c. The pulse-to-pulse amplitude fluctuation was generally less than 1.5% in root mean square (rms).

Figure 9a shows the average output power of the MOFA injected by the seed laser with $T_0 = 40\%$ as a function of launched pump power at a repetition rate of 25 kHz. It was found that the end facet damage of the fiber limited the maximum average output power to be approximately 4.8 W under the pump power of 10 W. As a result, the maximum pulse energy was restricted to 192 μJ. Figure 10 depicts the microscope image of the damaged end view and the side view of the fiber. Figure 9b shows the typical oscilloscope trace for a single pulse at the maximum output powers of amplifier. The pulse duration was 1.6 ns and the corresponding peak power was 120 kW. The calculated optical intensity on the end facet of the fiber was 27.2 J/cm^2 which agrees with the surface damage threshold of fused silica at 1064 nm [34]. The oscilloscope trace of a train of output pulses of the amplifier is shown in Fig. 9c. The pulse-to-pulse amplitude fluctuation was generally less than 4.0% in rms.

The timing jitters for both the amplifiers shown in Figs. 8 and 9 were generally less than 2% in rms. The M^2 factors were found to be smaller than 1.3 over the entire output power range. Furthermore, the polarization extinction ratios for both the amplifiers were measured to be about 100:1. Figures 11a and 11b show the optical spectra of the MOFAs at the maximum output powers injected by the seed lasers with $T_0 = 70$ and $T_0 = 40\%$, respectively. It can be seen that the peak levels of the amplified spontaneous emission (ASE) around 1040 nm shown in Figs. 11a and 11b were approximately 30 and 40 dB below the signal peak intensity, respectively. The power levels of the whole ASE intensities at the maximum output powers shown

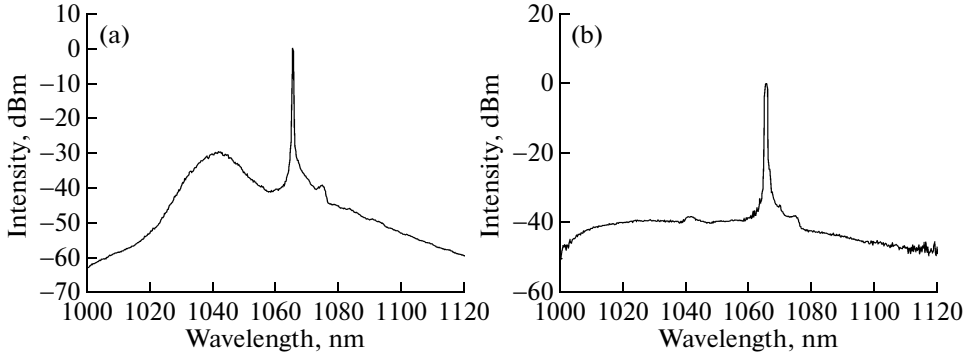

Fig. 11. Optical spectra of the MOFAs at the maximum output powers injected by the seed lasers with T_0 = (a) 70 and (b) 40%.

in Figs. 8a and 9a were measured to be less than 2% and 0.5%, respectively.

5. CONCLUSIONS

In conclusion, we have developed compact Nd:YVO_4/Cr^{4+}:YAG PQS lasers as seed oscillators for high-peak-power, single-stage, linear-polarized MOFAs. Compact and high-peak-power Nd:YVO_4/Cr^{4+}:YAG PQS lasers were theoretically optimized by considering the second threshold criterion and the thermal lensing effect in a nearly hemispherical cavity. Several Cr^{4+}:YAG crystals with different initial transmissions (T_0) have been used to confirm the performance of the designed PQS laser. It was experimentally found that at a pump power of 5.4 W the output pulse energy increases from 22 to 36 μJ and the pulse repetition rate decreases from 50 to 25 kHz for the initial transmission of the Cr^{4+}:YAG crystal decreasing form 70 to 40%. Injecting the seed laser obtained with $T_0 = 70\%$ into a polarization maintained Yb-doped fiber, the pulse energy and peak power at a pump power of 16 W were found to be 178 μJ and 37 kW, respectively. Employing the seed laser obtained with $T_0 = 40\%$, it was found that the surface damage of the fiber limited the maximum pulse energy and peak power to be 192 μJ and 120 kW, respectively. The polarization extinction ratio was approximately 100:1 for both MOFAs in the whole pump power. It is believed that the high peak-power and high polarization-extinction-ratio suggest further applications such as industrial material processing and nonlinear optics researches.

ACKNOWLEDGMENTS

The authors thank the National Science Council for the financial support of this research under Contract no. NSC-100-2628-M-009-001-MY3.

REFERENCES

1. E. Molva, Opt. Mater. **11**, 289 (1999).
2. Q. Liu, X. P. Yan, X. Fu, M. Gong, and D. S. Wang, Laser Phys. Lett. **6**, 203 (2009).
3. S. V. Garnov, V. I. Konov, T. Kononenko, V. P. Pashinin, and M. N. Sinyavsky, Laser Phys. **14**, 910 (2004).
4. L. Sun, L. Zhang, H. J. Yu, L. Guo, J. L. Ma, J. Zhang, W. Hou, X. C. Lin, and J. M. Li, Laser Phys. Lett. **7**, 711 (2010).
5. X. S. Cheng, B. A. Hamida, A. W. Naji, H. Ahmad, and S. W. Harun, Laser Phys. Lett. **8**, 814 (2011).
6. A. S. Kurkov, V. A. Kamynin, E. M. Sholokhov, and A. V. Marakulin, Laser Phys. Lett. **8**, 754 (2011).
7. X. Wushouer, P. Yan, H. Yu, Q. Liu, X. Fu, X. Yan, and M. Gong, Laser Phys. Lett. **7**, 644 (2010).
8. H. J. Liu and X. F. Li, Laser Phys. **21**, 2118 (2011).
9. Z. Y. Dong, S. Z. Zou, H. J. Yu, Z. H. Han, Y. G. Liu, L. Sun, W. Hou, X. C. Lin, and J. M. Li, Laser Phys. **21**, 1804 (2011).
10. Z. Y. Dong, S. Z. Zou, Z. H. Han, H. J. Yu, L. Sun, W. Hou, X. C. Lin, and J. M. Li, Laser Phys. **21**, 536 (2011).
11. C. Ye, P. Yan, L. Huang, Q. Liu, and M. Gong, Laser Phys. Lett. **4**, 376 (2007).
12. A. V. Kir'yanov, S. M. Klimentov, I. V. Mel'nikov, and A. V. Shestakov, Opt. Commun. **282**, 4759 (2009).
13. P. E. Schrader, R. L. Farrow, D. A. V. Kliner, J.-P. Feve, and N. Landru, Opt. Express **14**, 11528 (2006).
14. C. D. Brooks and F. Di Teodoro, Appl. Phys. Lett. **89**, 111119 (2006).
15. C. Li, J. Song, D. Shen, N. S. Kim, J. Lu, and K. Ueda, Appl. Phys. B **70**, 471 (2000).
16. Z.-Y. Li, H.-T. Huang, J.-L. He, B.-T. Zhang, and J.-L. Xu, Laser Phys. **20**, 1302 (2010).
17. J.-L. Li, D. Lin, L.-X. Zhong, K. Ueda, A. Shirakawa, M. Musha, and W.-B. Chen, Laser Phys. Lett. **6**, 711 (2009).
18. R. J. Lan, M. D. Liao, H. H. Yu, Z. P. Wang, X. Y. Hou, X. G. Xu, H. J. Zhang, D. W. Hu, and J. Y. Wang, Laser Phys. Lett. **6**, 268 (2009).
19. S. Y. Zhang, H. T. Huang, M. J. Wang, L. Xu, W. B. Chen, J. Q. Xu, J. L. He, and B. Zhao, Laser Phys. Lett. **8**, 189 (2011).
20. Y. Bai, N. Wu, J. Zhang, J. Li, S. Li, J. Xu, and P. Deng, Appl. Opt. **36**, 2468 (1997).
21. M. Liu, J. Liu, S. Liu, L. Li, F. Chen, and W. Wang, Laser Phys. **19**, 923 (2009).
22. Y. F. Chen, S. W. Tsai, and S. C. Wang, Opt. Lett. **25**, 1442 (2000).
23. F. Q. Liu, J. L. He, J. L. Xu, B. T. Zhang, J. F. Yang, J. Q. Xu, C. Y. Gao, and H. J. Zhang, Laser Phys. Lett. **6**, 567 (2009).
24. H. Yu, H. Zhang, Z. Wang, J. Wang, Z. Shao, and M. Jiang, Opt. Express **15**, 3206 (2007).
25. H. Yu, H. Zhang, Z. Wang, J. Wang, Y. Yu, M. Jiang, and X. Zhang, Opt. Commun. **281**, 5199 (2008).
26. H.-J. Qi, X.-D. Liu, X.-Y. Hou, Y.-F. Li, and Y.-M. Sun, Laser Phys. Lett. **4**, 576 (2007).
27. G. Xiao, J. H. Lim, S. Yang, E. Van Stryland, M. Bass, and L. Weichman, IEEE J. Quantum Electron. **35**, 1086 (1999).
28. A. Agnesi and S. Dell'Acqua, Appl. Phys. B **76**, 351 (2003).
29. Y. F. Chen, Y. C. Chen, S. W. Chen, and Y. P. Lan, Opt. Commun. **234**, 337 (2004).
30. N. Hodgson and H. Weber, *Laser Resonators and Beam Propagation*, 2nd ed. (Springer, Berlin, 2005), Ch. 5.
31. W. Koechner, *Solid-State Laser Engineering*, 6th ed. (Springer, Berlin, 2005), Ch. 7.
32. N. Hodgson and H. Weber, *Laser Resonators and Beam Propagation*, 2nd ed. (Springer, Berlin, 2005), Ch. 8.
33. Y. F. Chen, T. M. Huang, C. F. Kao, C. L. Wang, and S. C. Wang, IEEE J. Quantum Electron. **33**, 1424 (1997).
34. J. H. Campbell and F. Rainer, Proc. of SPIE **1761**, 246 (1992).